Identification of pests and diseases of Dalbergia hainanensis based on EVI time series and classification of decision tree

Qiu Luo[*,1], Wu Xin[2], XiongQiming[2]

[*,1]School of Geosciences and Info-Physics, Central South University, Hunan, Changsha, P. R. China
[2]Central South University of Forestry and Technology, Hunan, Changsha, P. R. China

*Email: 34489492@qq.com

Abstract. In the process of vegetation remote sensing information extraction, the problem of phenological features and low performance of remote sensing analysis algorithm is not considered. To solve this problem, the method of remote sensing vegetation information based on EVI time-series and the classification of decision-tree of multi-source branch similarity is promoted. Firstly, to improve the time-series stability of recognition accuracy, the seasonal feature of vegetation is extracted based on the fitting span range of time-series. Secondly, the decision-tree similarity is distinguished by adaptive selection path or probability parameter of component prediction. As an index, it is to evaluate the degree of task association, decide whether to perform migration of multi-source decision tree, and ensure the speed of migration. Finally, the accuracy of classification and recognition of pests and diseases can reach 87%--98% of commercial forest in Dalbergia hainanensis, which is significantly better than that of MODIS coverage accuracy of 80%--96% in this area. Therefore, the validity of the proposed method can be verified.

1 Introduction

Huanghuali wood, named *Dalbergia odorifera*, also known as *Dalbergia hainanensis*, is a kind of secondary national protected wild plants, on the brink of extinction. In the seeding and sapling stage, artificial cultivated Huanghuali wood is easily infected with anthracnose and tar spot disease, which result in a large number of leaves off, and seriously impact on the growth of young trees. Therefore, the rapid and timely grasp of the health status of Huanghuali wood is of great significance for carrying out precious tree cultivation. Traditional method of monitoring pests and diseases is mainly based on the visual investigation of artificial field, which requires a lot of manpower and material resources. So it cannot make a fast, objective and comprehensive dynamic assessment for the development of plant diseases and insect pest [1-5]. However, based on the remote sensing image analysis technology, the different remote sensing image of phase space can be used to extract and analyze the spectral signature of forests, and integrate the expert experience to realize the real-time monitoring and processing of pest information. Hence, compared with traditional monitoring methods of pest and disease, the new technology is provided with economical, macroscopical, and effective features [6-9].

At present, researchers at home and abroad have made many practical results in the research of monitoring pests and diseases, by using remote sensing satellite technology [10-15]. Royle, etc, for example, have used detective techniques of Landsat TM data and change for monitoring the health status of hemlock in New Jersey [16]. Based on the spectral signature index of TM remote sensing image, Chen has made an assessment and analysis of different levels of verticillium wilt in cotton [17].

Besides, based on the hyperspectral data of remote sensing, Jing has also obtained ideal effects in the construction of an evaluative model inversed by the severe level of verticillium wilt in cotton [18]. By studying the reflectance of stripe rust in the canopy of wheat, Guo, etc, have discovered that there is a directly proportional relation between the reflectance and disease level, which can be used as the characteristic basis of predicting stripe rust [19]. According to changes of needle spectrum in different course of nematodiasis, Xu has constructed an evaluative model for the disease of pine wood [20]. What's more, a correlation between PRI index and the yellow rust disease of winter wheat has been found in Huang W. J.'s research, according to which he has built an evaluative and predictive model [21].

On the basis of previous researches, this paper is mainly studied for pests' and diseases' recognition of commercial forest in *Dalbergia hainanensis*. Then, considering phenological features, it has designed and realized recognition methods of pests and diseases for *Dalbergia hainanensis* based on EVI time-series and the classification of decision tree of multi-source branch similarity. As a result, the purpose of this paper is used to prevent and control the pest and disease of *Dalbergia hainanensis*, as well as forest cultivation.

2 Site description

Hainan Jian Fengling National Forest Park was founded in 1992. As the first National Forest Park built in Hainan, the park, an area of 447 km2, is located in southwest of Hainan Island and stretched across East and Le Dong two administrative regions. This area has the most complete and largest, as well as the highest biological diversity of pristine tropical rainforest, and its coverage rate of forest vegetation get up to 98%. Meanwhile, it is the main concentration of commercial forest in *Dalbergia hainanensis*. So how to monitor and prevent the commercial forest of Huanghuali wood quickly and effectively has very an important economic value, due to the complex terrain and vegetation.

In short, this paper is to conduct an accurate assessment of pests and diseases by anthracnose and tar spot disease as research objects. Then, h25v03 of 2013 strip number and a resolution of 500m of remote sensing data (MOD13QI) are to be selected in Huanghuali wood area of Jian Fengling National Park in Hainan Province.

3 Research ideas and methods

In this study, identification of pests and diseases of *Dalbergia hainanensis* based on EVI time-series and classification of decision tree mainly includes several steps, such as remote sensing data reading, data preprocessing, classification and gradation of pests and diseases, etc. Specific work process is shown in figure 1.

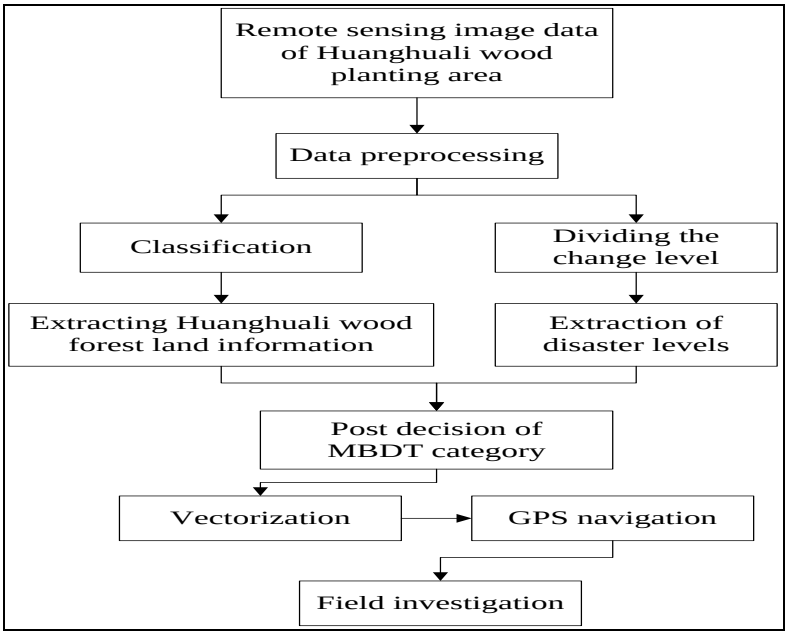

Figure 1: Identification process of pests and diseases of *Dalbergia hainanensis*

3.1 Parameter extraction of phonological features

In this study, TIMESAT toolkit of MATLAB platform is used to process remote sensing image of commercial forest in Huanghuali wood area. Double logistic function is fitting constructed EVI time-series data. In order to obtain the growth law information of seasonal vegetation, TIMESAT toolkit, is developed both by Jonsson and Eklundh, as a software package for the reconstruction of time-series data set on vegetation index, and extraction of phenological information on vegetation growth [22].

The extraction of phonological parameters [23,24] of commercial forest in Huanghuali wood area mainly involves the start and end of season (SOS, EOS), length of season (LOS), max of EVI (MOE), as well as amplitude of EVI (AOE). In the start and end of season of Huanghuali wood, significant variation characteristics of EVI index can be organically combined with actual research needs. In the experiment, a midpoint is selected between the minimum and maximum of EVI, which is treated as the start and end of growth season of Huanghuali wood. Besides, based on the gained double Logistic function [25-27] fitting, difference between the maximum and corresponding function of Huanghuali wood EVI growing season is selected as its amplitude of EVI. The objective is to minimize the variance between the sample of each disease course and the acquired parameter of phonological features.

3.2. Similarity decision-tree of multi-source branch

3.2.1 Similarity measure of decision-tree. For remote sensing data set$\boldsymbol{D}$, the attribute space of which is$\boldsymbol{R^n}$, and $\mathbf{n}$is the number of spatial attribute. Decision tree$\boldsymbol{DT}$is able to divide the space $\boldsymbol{R^n}$ into $\boldsymbol{Q}$different regions, where the class label for each region $\boldsymbol{r_m}$is$\boldsymbol{r_{m.cl}}$. Therefore, decisiontree$\boldsymbol{DT}$acts similarly to the constant piecewisefunction $\boldsymbol{f_{DT}}: \boldsymbol{x} \rightarrow \boldsymbol{r_{m.cl}}$. The correspondinglabel value$\boldsymbol{r_{m.cl}}$is tobe outputted after the corresponding relation between the sample$\boldsymbol{x} \in \boldsymbol{D}$and its corresponding region$\boldsymbol{r_m}$.

Generally speaking, for the forecasting decision-making area r, there are two kinds of structural forms to express, the actual path and composition. And the path structure$r.p$can be described by the following formula.

$$r \cdot p = \{\cap\, d(a_v), v = 1,2,\cdots K_r\} \quad (1)$$

In the formula (1), $d(a_v)$ is the value range of the attribute$a_v$in the corresponding region$r$. $K_r$is the total number of nodes appearing in the path of root node of region$r$. Then, the symbol of "∩" is the intersection between the existence of overlapping relation. "$r \cdot p$" is the path structure, whose value

reflects the association structure between the decision tree $DT$and the prediction region r. And the structure shows the attribute rule set of region$r$and its root node.

In order to describe the data set$D$contained in the region r, r component is assumed as the following form.

$$r \cdot c = \{num(k_1), num(k_2), \cdots num(k_J)\} \quad (2)$$

In Formula (2), J represents the total number of categories. Entering parts of the area r , $num(k_1), num(k_2), \cdots, num(k_J)$ belongs to the sample quantity of $k_1, k_2 \cdots, k_J$ different categories. While, the component structure $r \cdot c$ represents the relation component between the prediction region$r$ and its corresponding data set D. Two decision trees $DT_1$and DT_2, which are related but have different structures, can describe their similarities by the existing affinity coefficient based on the probabilistic prediction of the sample. Based on the accessibility of training data, probability prediction$P(r)$can be constructed into two index, the predictive component probability $P(r \cdot c)$ and the predictive path probability$P(r \cdot p)$. Its corresponding form of calculation is shown as formula(3) and (5) [28].

$$P(r_m \cdot p) = \frac{V(r_m \cdot p)}{\sum_{l=1}^{Q} V(r_l \cdot p)} \quad (3)$$

$$\mathrm{V}(r_m \cdot p) = \prod_{v=1}^{K_{r_m}} \frac{|d(a_v)|}{|dom(a_v)|} \quad (4)$$

$$P(r_m \cdot c) = \frac{|r_m \cdot c|}{\sum_{l=1}^{Q} |r_l \cdot c|} \quad (5)$$

Formula (4) represents the area super-volume ofr_m after normalizationoperation in the attribute spaceR^n. $|dom(a_v)| = max(a_v) - min(a_v)$, this formula is for the value of attributea_v in the global scope. $|d(a_v)| = max_{r_m}(a_v) - min_{r_m}(a_v)$, this formula indicates the range of a_v's value within a given region r_m.$|r_m \cdot c| = \sum_{\rho=1}^{J} num(k_\rho)$, formula (5) shows the sum of different samples in the region r_m.

It needs attention that the predicted path probability $P(r \cdot p)$must accord with the assumption of consistent distribution based on formula (3). If not satisfied, it will result in serious deviation. Therefore, generally speaking, formula (5) should be selected to obtain the prediction probability as much as possible except the original training set$D$inaccessible. In addition, formula (3) and (5) only give component predition, and the complete prediction probability form is shown as follows: $P(r) = \{P(r_m) | m = 1,2, \cdots, Q\}$.

After obtaining$P(r)$, the similarity of the decision tree can be calculated based on the following equation [29]:

$$S(DT_1, DT_2) = s\big(P_{DT1}(r), P_{DT2}(r)\big) = \sum_{m=1}^{Q} [P_{DT1}(r_m) \cdot P_{DT2}(r_m)] \quad (6)$$

In formula (6), $S(\cdot,\cdot)$ denotes the affinity coefficient between decision trees, and its expansion form is shown as the right side of this formula. This formula reflects the approximate degree of different distributive probability and meets the relationship$0 < (\cdot,\cdot) \leq 1$. Besides, if values of$S(DT_1, DT_2)$are in the range of $(0, 1]$ and DT_1 and DT_2 have similar values of the probabilistic prediction, values of$S(DT_1, DT_2)$ are close to 1, or close to 0. When only the equation $P_{DT_1}(r) = P_{DT_2}(r)$ is satisfied, there exists $S(DT_1, DT_2) = 1$.

3.2.2 Decision tree migration of multi-source branch. For the multi-source learning transfer process, the formis $\boldsymbol{KT}: \boldsymbol{S_1}\times\boldsymbol{S_2}\times\cdots\times\boldsymbol{S_N}\rightarrow\boldsymbol{T}$, $\boldsymbol{S_i}(\boldsymbol{i}=\boldsymbol{1},\boldsymbol{2},\cdots,\boldsymbol{N}$ indicates the source task, $\boldsymbol{T}$ indicates task object. Then, different situations of $\boldsymbol{S_i}$ correspond to the source decision tree $\boldsymbol{DT_i}$, and its algorithm systemic structure is shown in figure 2. The algorithm is divided into three stages, namely, the decision tree training of source domain, similarity discrimination, and multi-source integration migration. According to the accessibility of the source domain data set, the mechanism of similarity discrimination can be divided into two constituent mechanisms: composition and path. As is shown in figure 2 phase 2, the structure of discriminate branches can be abbreviated in forms STDT-C and STDT-P respectively.

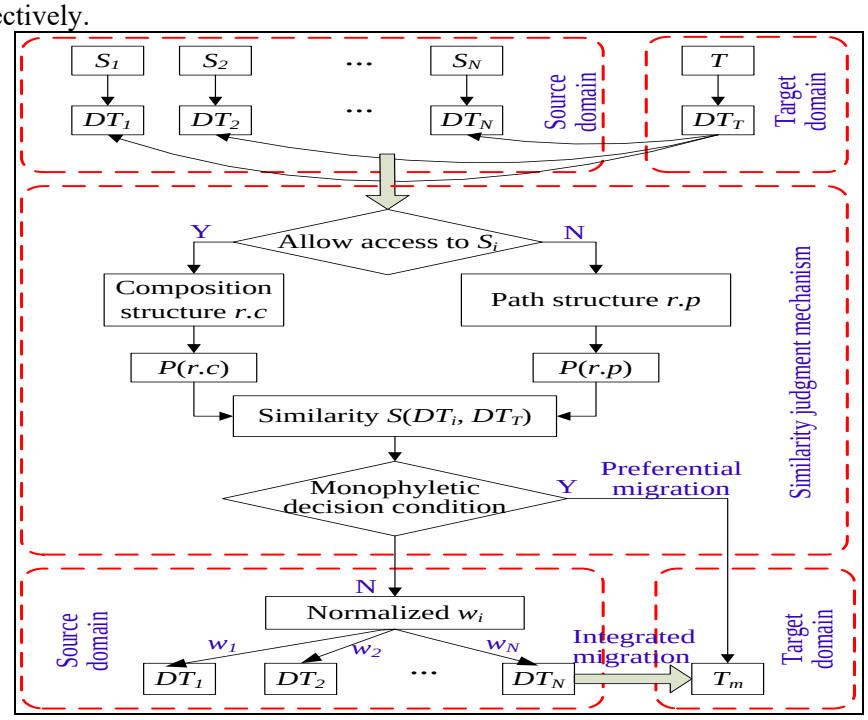

Figure 2: Migration system structure of the multi-source branch decision tree

Each source task S_i by using the decision tree DT has the following mathematical descriptive form [30]:

$$g(k|x) = P(k|x) + e_k(x) \qquad (7)$$

*P(k/x)*inside is the sample x belonging to the ideal experimental probability of K class. Then, $e_k(x)$ is the estimated error of the source task S_i. And $g(k|x)$ indicates that x belongs to the estimated probability of$k$ class.

In order to obtain the corresponding migration between the target task T and the multi-source task S_i, T is supported by aid decision making based on the linear combination. That is,

$$gT(k|x) = \sum_{i=1}^{N} w_i g_i\,(k|x) = P(k|x) + e_k^T(x) \qquad (8)$$

Compared with formula (7), the result is $e_k^T(x) = \sum_{i=1}^{N} w_i e_k^i(x)$.

For how to determine the migration weight w_i, it can be measured by the similarity between the different source decision tree DT_i and the target decision tree DT_T. Taking the equation$\sum_{i=1}^{N} w_i = 1$into consideration, there is:

$$w_i = \left[\sum_{q=1}^{N} S(DT_q, DT_T)\right]^{-1} S(DT_i, DT_T) \qquad (9)$$

3.2.3 Calculation process. Step1: (prior knowledge) from the source decision tree DT_i by the training of various source data set S_i in the source domain [31,32], training set of the target domain, as well as the target decision-making task DT_T.

Step 2: (determination in sequence) calculating the similarity [33] $S(DT_i, DT_T)$ between DT_T and each source target task DT_i. If the data set in the source domain can be accessed, the structural

component $r \cdot c$ of region r is calculated based on formula (2). Then, the predictive component probability $P(r \cdot c)$ is obtained based on formula (5), or the path structure $r \cdot p$is gained based on formula (1). The path prediction probability $P(r \cdot p)$ is calculated by formula (3).

Step 3: Determine whether the monophyletic migration condition is met. If meet, selecting the largest DT_i in $S(DT_i, DT_T)$ is to perform the migration operation and execute the decision on the task target. Otherwise, proceed to step 4.

Step 4: Normalize the similarity of $S(DT_i, DT_T)$ and obtain the corresponding migration weightw_i, which is assigned to decision trees of the source domain in turn.

Step 5: Perform the integrated migration operation based on the linear combination [34,35], that is, to obtain the decision-tree of task target $DT_T = \sum_{i=1}^{N} w_i \cdot DT_i$, the algorithm terminates.

4 Experimental results and analysis

4.1 Grade classification of pests and diseases of Huanghuali wood

Based on the field investigation, samples of pests and diseases is obtained and used to generate the interest research area. At the resolution ratio of 250 m, there are a large number of mixed pixels. Though each pixel cannot guarantee the uniformity of the distribution of pests and disease of Huanghuali wood, it is accurate to the grade distribution of pests and diseases by the way of decision tree. Meanwhile, the concentration of information is increased by using phonological feature information based on the grade distribution. According to four grades of pests and diseases of Huanghuali wood, 100 remote sensing pixel and 5 phenological feature parameters are selected in radon to execute the analysis of phenological feature on pests and diseases.

For all selected phonological feature parameters, 100 group of pixel sample points as samples from 4 kinds of pests and diseases are to perform a scatter graph. Based on the fitting analysis of phonological parameters, SOS characteristic values of Huanghuali wood are differed in different grades of pests and diseases. However, AOE values of diseased and non-diseased plants are significantly different at 0.4. For example, the index range for the severe pests and diseases of Huanghuali wood is $EOS > 275 \&\& MOE > 0.4$, for moderate is$SOS > 155 \&\& MOE > 0.4 \&\& AOE > 0.4$, and for the mild is$SOS > 140 \&\& AOE > 0.4$. Therefore, according to the above selected threshold to achieve the effect of differentiation, feature 3 is the criteria of classification on pests and diseases of Huanghuali wood, based on the extraction of the start time and EVI amplitude in its growth season.

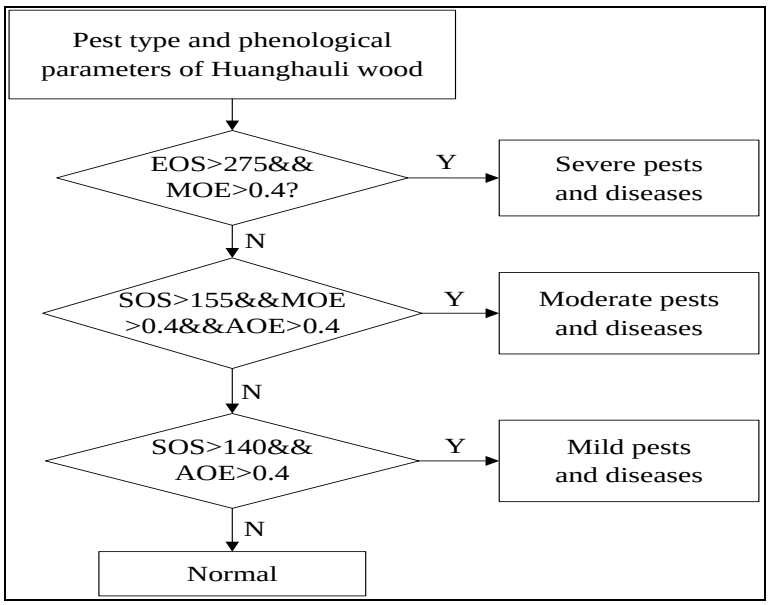

Figure 3: Grade classification of pests and diseases of Huanghuali wood

4.2 Diseases fitting of EVI time-series

Based on the most approaching algorithm, the remote sensing data of 500m resolution is interpolated into 250m remote sensing data, which is achieved one-to-one pixel correspondence to the result of this study on the grade recognition of pests and diseases. The fitting result of phonological features is shown in figure 4.

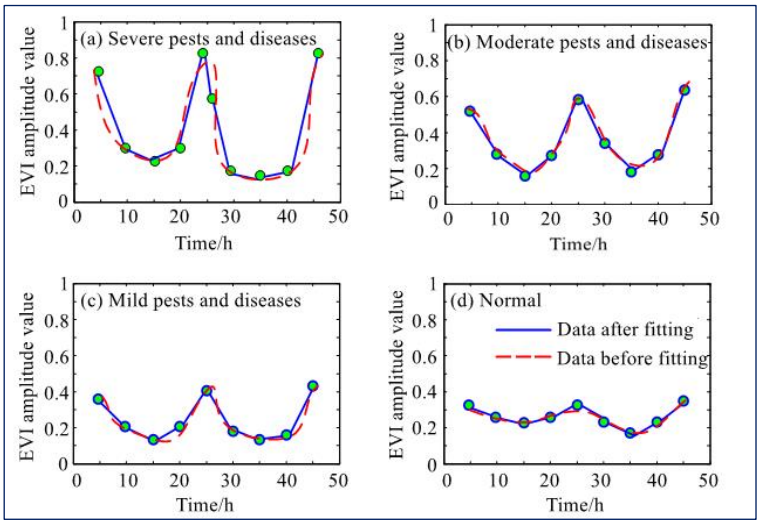

Figure 4: Disease types and fitting results

In this paper, a double logistic function is adopted. This fitting way can effectively reflect phenological features of vegetation difficult to directly extract, which is equivalent to performing a filtering operation for EVI time-series data. Therefore, the noise can be shielded and phenological features of pests and diseases of Huanghuali wood are to be prominent. Figure 4 shows comparison results of EVI time-series curve data, which four types of grades of pests and diseases are implemented before and after the filtering operation. Comparing curves gained before and after the filtering operation can be seen that the double Logistic function fitting is effectively in shielding the original EVI time-series curve [36]. Moreover, it can be effectively approaching, make smoother curve, and highlight phenological features of Huanghuali wood reflected by EVI time-series curve. From the EVI time-series curve on diseases of 4 types of this wood in figure 4, it can be seen that different plants have evident differences on indexes of length, the beginning and ending time, as well as the EVI time-series amplitude in the growing season, etc.

4.3 Identification results of pests and diseases of Dalbergia hainanensis

Figure 5 shows the remote sensing image and identification results of similarity decision trees of the multi-source branch on pests and diseases of Huanghuali wood area in Jian Fengling National Forest Park. Both mild and severe two label forms are given in this picture. Besides, it also shows in figure 5 that the identification of this kind of decision tees can identify the extent of disease accurately and has high accuracy in the mild and severe identification of pests and diseases.

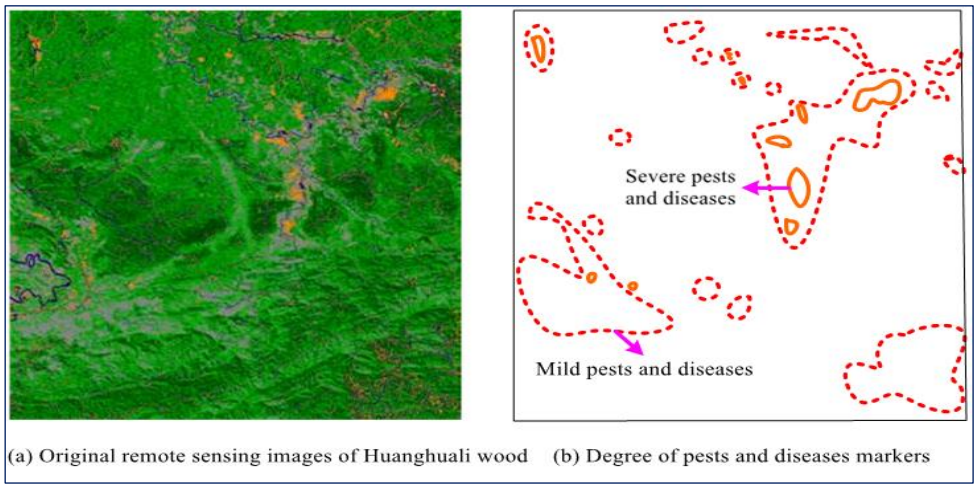

Figure 5: Degree of pests and diseases markers (the mild and severe)

For each of 4 types of pests and diseases, 300 sample points are randomly sampled to verify the result of grade identification of pests and diseases, the classification accuracy evaluation, the confusion matrix, the grade accuracy evaluation, and the experimental data of confusion matrix respectively, as shown in table 1 and figure 6.

Table 1 shows results of accuracy comparison of MODIS and MBDT algorithm in the classified identification of disease degree. Then, it can be seen that differences between the identification accuracy of these two algorithms are relatively small in severe and normal two levels, while, identification accuracy of MODIS algorithm is low in mild and severe identifications. As a result, MBDT algorithm has higher identification in this paper.

Table 1: Comparison of classification accuracy

Degree of pests and diseases	MBDT	MODIS
Severe	93.6	90.6
Moderate	87.4	80.1
Mild	91.8	82.7
Normal	97.6	95.4

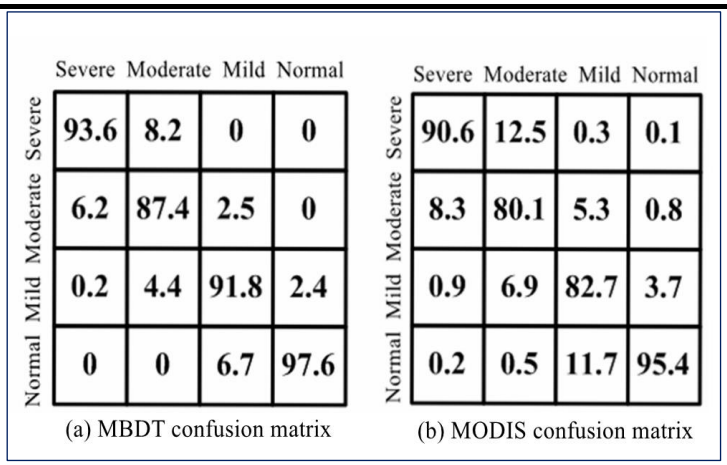

Figure 6: Confusion matrix comparison

From the confusion matrix in figure 6, MBDT algorithm in this paper has a big confusion in moderate and severe degrees. Though there is some confusion in mild and normal degree, the overall

confusion rate is low. Compared with the confusion matrix of MODIS algorithm, there is a certain degree of confusion between different levels, and recognition of the algorithm is relatively worse than MBDT algorithm.

5. Conclusion

Based on EVI time-series data indicators of similarity decision trees of multi-source branch, and combined with the fitting filtering method of Logistic function, this paper is to achieve an accurate prediction for pest and disease levels of 4 kinds of Huanghuali wood, which can be used to guide the preventive treatment of pests and diseases in forest. Meanwhile, there is of more ideal classified effect on the basis of grade identification for decision trees of phenological features. Based on EVI time-series index data, information extraction and analysis of phenological features are provided with high reliability for predicting pest and disease grades of Huanghuali wood.

However, phenological features obtained by the simple EVI index are not able to fully reflect the grade characteristics of pests and diseases of Huanghuali wood. And phenological features of this similar vegetation are also different in time and space. Phenological features of this wood are combined with non-remote sensing measured data, and with full consideration of environmental factors, such as precipitation and temperature on the phenological change, etc. Consequently, it is conducive to further improving the identification accuracy of pests and diseases of Huanghuali wood, which will be the focus in our future work.

Acknowledgements

We express our thanks to the anonymous referees for their valuable comments, which led to a significant improvement over an early version of the paper. And we gratefully acknowledge the help of Professor Zhang Gui, who has offered us valuable suggestions in the academic studies. We also like to express our gratitude to Yang Zhigao and Yu Deqing for their assistance in the field work.

References

[1] Chengfeng, L. "Forecast and control of main forest diseases and pests in south china″. Beijing: China Forestry Publishing, pp. 36- 95, (2003).

[2] Linke, J.; Fortin, M.J.; Courtenay, S.; Cormier, R. "High-resolution global maps of 21st-century annual forest loss: Independent accuracy assessment and application in a temperate forest region of atlantic canada", *Remote Sens Environ,* **188**, pp. 164- 176, (2017).

[3] Liu, Z.; Yan, M.; Zhang, X.; Gang, T.U. "Methodical study on monitoring wide-range forest insect pest by meteorsat", *Journal of Natural Disasters*, **11**, pp. 109-114, (2002).

[4] Nunoo, E.K.; Twum, E.; Pannin, A. "A criteria and indicator prognosis for sustainable forest management assessments: Concepts and optional policy baskets for the high forest zone in ghana", *J Sustain Forest*, **35**, pp. 149-171, (2016).

[5] Stenlid, J. "Emerging diseases in european forest ecosystems and responses in society", *Forests*, **2**, pp. 86-504, (2011).

[6] F., L. "Diseases and insect pests area monitoring for winter wheat based on hj-ccd imagery",*Transactions of the Chinese Society of Agricultural Engineering ,***26**, pp. 213- 219, (2010).

[7] J., Z.; L., Y.; J., W. "Research progress of crop diseases and pests monitoring based on remote sensing", *Transactions of the Chinese Society of Agricultural Engineering,* **28**, pp.1 - 11,(2012).

[8] Lili, Y.; Qingshu, L.; Ruozhong, J. "Research progress of remote sensing technology in forest pests and diseases detection", *Journal of Liaoning Forestry Science & Technology*, pp. 40- 44, (2012).

[9] N., R.A.; J., N. "Defection of mountain pine beetle infestation using landsat mss and simulated thematic mapper data", *Canadian Journal of Remote Sensing,* **11**, pp. 50- 58, (1985).

[10] Diofantos, H.G.; Panayiotis, P. "A national system for monitoring the population of agricultural pests using an integrated approach of remote sensing data from in situ automated

traps and satellite images", *Proceedings of SPIE - The International Society for Optical Engineering*, **7824**, pp. 375-387, (2010).

[11] G., L.D. "Factors affecting defoliation assessment using airborne multispectral scanner data", *Photogrammetry Engineering and Remote Sensing,* **53**, pp. 1665- 1674, (1987).

[12] Luo, J.; Huang, W.; Zhao, J.; Zhang, J.; Ma, R.; Huang, M. "Predicting the probability of wheat aphid occurrence using satellite remote sensing and meteorological data",*Optik - International Journal for Light and Electron Optics,* **125**, pp. 5660-5665, (2014).

[13] Okuyama, T.; Yang, E.C.; Chen, C.P.; Lin, T.S.; Chuang, C.L.; Jiang, J.A. "Using automated monitoring systems to uncover pest population dynamics in agricultural fields", *Agricultural Systems,* **104**,, pp.666-670,(2014).

[14] Wu, T.; Zhang, L.; Peng, B.; Zhang, H.; Chen, Z.; Gao, M. "In Real-time progressive hyperspectral remote sensing detection methods for crop pest and diseases″, *SPIE Commercial + Scientific Sensing and Imaging*, p 98，74，10, (2016).

[15] Zhang, M.; Qin, Z.; Liu, X.; Ustin, S.L. "Detection of stress in tomatoes induced by late blight disease in california, USA, using hyperspectral remote sensing",*International Journal of Applied Earth Observation & Geoinformation,* **4**, pp.295-310, (2003).

[16] D.D., R.; G., L.R. "Monitoring hemlock forest health in new jersey using landsat tm data and change detection techniques", *Forest Science Forest Science* **43**, pp. 327- 335,(1997).

[17] Bing, C.; Shaokun, L.; keru, W. "Estimating severity level of cotton disease based on spectral indices of tm image", *Journal of Infrared Millim. Waves,* **30**, pp.451- 457,(2011).

[18] Xia, J.; Wenjiang, H.; Jihua, W. "Hyper spectral inversion models on verticillium wilt severity of cotton leaf", *Spectroscopy and Spectral Analysis* **29**, pp. 3348- 3352,(2009).

[19] GuoJiebin, H.c., Wang Haiguang. "Disease index inversion of wheat stripe rust on different wheat varieties with hyper spectral remote sensing", *Spectroscopy and Spectral Analysis,* **29**, pp. 3353- 3357, (2009).

[20] Xu Huachao, L.Y., Zhang Tingting. "Changes of reflectance spectra of pine needles in different stage after being infected by pine wood nematode". *Spectroscopy and Spectral Analysis,***31**, pp. 1352- 1356,(2011).

[21] Huang W J, L.D.W., Niu Z. "Identification of yellow rust in using in-situ spectral reflectance measurements and airborne hyperspectral imaging", *Precision Agriculture*,**8**, pp.187-197,(2007).

[22] P., J.; L., E. "Timesat-a program for analyzing time-series of satellite sensor date", *Computers &Geosciences*, pp. 833- 845,(2004).

[23] Jonsson, P.; Eklundh, L. "Seasonality extraction by function fitting to time-series of satellite sensor data", *Geoscience & Remote Sensing IEEE Transactions on,* **40**, pp. 1824-1832,(2002).

[24] Kaufman, Y.J.; Tanré, D. "Atmospherically resistant vegetation index (arvi) for eos-modis", *IEEE Transactions on Geoscience & Remote Sensing,* **30**, pp. 261-270,(1992).

[25] Lipovetsky, S. "Double logistic curve in regression modeling", *Journal of Applied Statistics,***37**,pp. 1785-1793,(2010).

[26] Song, C.Q.; Ling-Hong, K.E.; You, S.C.; Liu, G.H.; Zhong, X.K. "Comparison of three ndvi time-series fitting methods based on timesat——taking the grassland in northern tibet as case", *Remote Sensing Technology & Application,* **26**, pp.147-155,(2011).

[27] Yang, X.; Mustard, J.F.; Tang, J.; Xu, H. "Regional-scale phenology modeling based on meteorological records and remote sensing observations", *Journal of Geophysical Research Biogeosciences,***117**, (2015).

[28] Mihalkova, L.; Huynh, T.; Mooney, R.J. "In Mapping and revising markov logic networks for transfer learning″, *National Conference on Artificial Intelligence*, pp 608-614,(2007).

[29] Quinlan, J.R. "Simplifying decision trees", *Massachusetts Institute of Technology*, (1986).

[30] Ntoutsi, I.; Kalousis, A.; Theodoridis, Y. "In A general framework for estimating similarity of datasets and decision trees: Exploring semantic similarity of decision trees″, *Siam International Conference on Data Mining*, Atlanta, pp. 810-821,(2008).

[31] Fumera, G.; Roli, F. "A theoretical and experimental analysis of linear combiners for multiple classifier systems", *IEEE Transactions on Pattern Analysis & Machine Intelligence,* **27**, pp. 942-956, (2005).
[32] Bailey, T.L.; Elkan, C. "The value of prior knowledge in discovering motifs with meme", **3**, pp.21-29, (1995).
[33] Thompson, M.L.; Kramer, M.A. "Modeling chemical processes using prior knowledge and neural networks", *Aiche Journal,* **40**, pp. 1328-1340, 1994.
[34] Tanaka, A. "Computer for calculating the similarity between patterns", US,(1984).
[35] Hashem, S. "Optimal linear combinations of neural networks", *Neural Networks,* **10**, pp. 599-614,(1997).
[36] Ullman, S.; Basri, R. "Recognition by linear combinations of models", *IEEE Transactions on Pattern Analysis & Machine Intelligence,* **13**, pp. 992-1006,(1989).
[37] Zhao, H.R.; Tang, Z.S. "A new filtering method based on spatial clustering", *Journal of Computer Applications,* (2006).